Morphology, Rheological, Crystallization Behavior, and Mechanical Properties of Poly(L-lactide)/Ethylene-*co*-Vinyl Acetate Blends with Different VA Contents

Yanli Li, Li Liu, Yunyun Shi, Fangming Xiang, Ting Huang, Yong Wang, Zuowan Zhou

Key Laboratory of Advanced Technologies of Materials (Ministry of Education), School of Materials Science and Engineering, Southwest Jiaotong University, Chengdu 610031, Sichuan, China

Received 9 August 2010; accepted 10 October 2010
DOI 10.1002/app.33581
Published online 29 March 2011 in Wiley Online Library (wileyonlinelibrary.com).

ABSTRACT: Poly(L-lactide)/ethylene-*co*-vinyl acetate (PLLA/EVA) blends with different contents of Vinyl Acetate (VA) in EVA phase were prepared through melt blending process. Although the composition of the blends was invariant (70/30), different phase morphologies were observed, namely, sea-island morphologies for the blends with VA contents of 7.5, 18, and 28 wt %, whereas approximate co-continuous morphology for the blend with VA content of 40 wt % was observed. The interfacial interaction between PLLA and EVA was visualized by Fourier transform infrared and rheological measurements. The nonisothermal and isothermal crystallization behaviors of the blends were investigated by wide angle X-ray diffraction, Differential scanning calorimetry, and polarization optical microscope. Post-thermal treatment was applied to improve the crystalline structure of PLLA. The results show that all the samples are mainly in amorphous state during the injection molding process. However, annealing promotes the second crystallization of PLLA matrix, leading to the improvement of the crystalline structure. Especially, the effect of annealing on crystalline structure of PLLA matrix is greatly dependent on the VA content of EVA. As expected, addition of EVA results in the improvement of the ductility and fracture toughness of the blends. The decreased tensile modulus and tensile strength can be enhanced through annealing process. © 2011 Wiley Periodicals, Inc. J Appl Polym Sci 121: 2688–2698, 2011

Key words: PLLA/EVA; microstructure; rheological; crystallization; mechanical properties

INTRODUCTION

Poly(L-lactide) (PLLA) is one of the biodegradable and biocompatible polymers and has received increased attention in the decades due to its comprehensive mechanical properties. Similar to other semicrystalline polymers, the properties of PLLA, including the mechanical behavior, thermal properties, and degradation profile, are strongly dependent on the degree of crystallinity [X_c(%)] and crystalline morphology.[1–3] However, the crystallization of PLLA is very slow to develop significant crystallinity, especially, during the normal processing involved the nonisothermal conditions, such as extrusion and injection molding, it is hard to achieve high X_c(%) in PLLA. In this case, the amorphous content of PLLA plays a very important role on the final properties of the particles. Consequently, the fracture toughness is very poor, and the particles are brittle and very sensitive to the environment stress and other impact load. On the other hand, the processability of PLLA is inferior to that of the polyolefin. Thus, the wide application of PLLA in packaging, which needs a certain degree of ductility, is greatly limited.

Blending with plasticizer is now widely adopted in modification of PLLA materials due to the dual effects of plasticizer in PLLA. Plasticizer can greatly improve the mobility of PLLA chain segments, and consequently, the glass transition temperature (T_g) of PLLA is decreased, and the crystallization is improved greatly on the one hand.[3–6] On the other hand, the presence of plasticizer improves the processability and ductility of PLLA greatly.[7] However, large reduced tensile strength and Young's modulus have been reported simultaneously due to the decrease of the macromolecular chain cohesion density.[7,8]

Recently, blending PLLA with other polymers has been the main subject of many researches. The studies on PLLA blends are mainly focused on the miscibility[9–12] and rheological properties.[13–16] However, less work has been done to investigate the toughening of PLLA by elastomers.[17–19] Ishida[17] added four

Correspondence to: Y. Wang (yongwang1976@163.com).
Contract grant sponsor: National Natural Science Foundation of China; contract grant number: 50973090.
Contract grant sponsor: Program for New Century Excellent Talents in University; contract grant number: NCET-08-0823.
Contract grant sponsor: Sichuan Youthful Science and Technology Foundation; contract grant number: 07ZQ026-003.

TABLE I
Polymers Used in This Study

Materials	Trade work	VA content (wt %)	Density (g cm^{-3})	MFR (g/10 min)	T_m (°C)	Manufacturer
PLLA	2002D	–	1.24	4–8		Nature works
7.5EVA	Elvax 3120	7.5	0.93	1.2	97.0	Dupont
18EVA	Elvax 460	18.0	0.94	2.5	85.8	Dupont
28EVA	Elvax 265	28.0	0.95	3.0	72.5	Dupont
40EVA	Elvax 40L-03	40.0	0.97	3.0	58.8	Dupont

different elastomers into PLLA and found that the smaller the dispersed particles are, the better the impact strength is. They also suggested that elastomer with a high polarity is more suitable for toughening PLLA. Li[18] investigated the toughening effect of acrylonitrile-butadiene-styrene copolymer on PLLA and found that the blends exhibit poor mechanical properties with low elongation at break and decreased impact strength due to the poor miscibility. Other work has proved that linear low-density polyethylene exhibits toughening effect for PLLA to a certain extent.[20,21]

In this work, we attempted to study the effect of elastomer on microstructure, rheological, and mechanical properties of PLLA. Four kinds of ethylene-*co*-vinyl acetate (EVA) with different contents (7.5, 18, 28, and 40 wt %) of VA monomer in EVA phase were used. It is already proved that poly(vinyl acetate), which has the similar monomer with the comonomer of EVA, is miscible with PLLA.[22] For EVA, it has been reported that when the VA content is more than 85 wt %, EVA is miscible with PLLA.[23] Thus, it is expected that with the variation of VA content, the interaction between PLLA and EVA changes correspondingly. Especially, the crystallization behavior of EVA self deteriorates, and the melting temperature (T_m) decreases with the increase of VA content. This possibly results in the different effects of EVA on microstructure of PLLA during the post-treatment. Similar to other brittle polymers toughened by elastomer, the strength and stiffness of PLLA blends will deteriorate inevitably. Thus, the post-thermal treatment, that is annealing, will be carried out for PLLA blends. Annealing is thought to be one of the best ways to improve the mechanical properties of PLLA through promoting the second crystallization of PLLA, which increases the X_c (%) and chain relaxation of PLLA.[21,24–29] Thus, it is expected that PLLA blends with comprehensive mechanical properties will be achieved through blending of EVA and post-thermal treatment.

EXPERIMENTAL

Materials

All the materials used in this study are commercially available. PLLA (2002D, D-isomer content = 4.3%, $M_w = 2.53 \times 10^5$ g mol^{-1}, melt flow rate = 4–8 g/10 min (190°C/2.16 kg), and density of 1.24 g cm^{-3}) was purchased from NatureWorks®, Minnetonka, USA. Four kinds of EVA with different VA contents were purchased from DuPont Industrial Polymers, Wilmington, USA. The main information about the EVA is shown in Table I.

Sample preparation

PLLA (70 wt %) and EVA (30 wt %) were melt-blended using a twin-screw extruder (SHJ-20, China). The selection of this composition is expected that the blends with different contents of VA in EVA phase will exhibit apparent variations in morphologies, that is, from sea-island to co-continuous morphologies. During the extrusion, the screw speed was set as 120 rpm, and the temperature was 130–190°C from hopper to die. After making droplets, the pellets were injection molded using an injection-molding machine (PS40E5ASE, Japan) at the melt temperature of 190–210°C and the mold temperature of 23°C. Some injection-molded bars were directly characterized, and others were first annealed at 80°C for 1 h and then were characterized to know the effect of thermal treatment on the microstructure and mechanical properties of the blends. It has been proved in our previous work that annealing temperature has great influence on the second crystallization behavior of PLLA.[28,29] At relatively lower temperature, for example, 60°C, the second crystallization behavior of PLLA is greatly limited and annealed PLLA samples are still in the amorphous state. However, at relatively higher temperature (>100°C), as the chain segments mobility is greatly improved, and the second crystallization of PLLA occurs easily, pure PLLA exhibits similar crystalline structure with PLLA nanocomposites and/or blends. In this condition, the effect of nanofiller and/or plasticizer on second crystallization of PLLA during annealing becomes inconspicuous, and PLLA nanocomposites and or blends exhibits similar crystalline structure with pure PLLA. Thus, to show the different effects of EVA with different contents of VA monomer on second crystallization of PLLA clearly, the moderate annealing temperature, 80°C, was adopted in this work.

Fourier transform infrared

The interaction between PLLA and EVA was investigated using Fourier transform infrared instrument (FTIR, Nicolet 5700, USA) from 4000 cm^{-1} to 400 cm^{-1} at a resolution of 4 cm^{-1}.

Scanning electron microscope

The phase morphologies of the blends were characterized using a Fei Inspect F high-resolution scanning electron microscopy (SEM, The Netherlands) with an accelerating voltage of 2.0 kV. Before characterization, the sample was cryogenically fractured in liquid nitrogen, and the fractured surface was coated with a thin gold layer. The SEM photographs were analyzed using an image analyzer to calculate the diameter of dispersed phase. A minimum number of 200 dispersed particles were considered. The weight average EVA particles diameter ($\overline{d}_w$) was calculated using the following equation:

$$\overline{d}_w = \sum n_i d_i^2 \Big/ \sum n_i d_i \tag{1}$$

where n_i is the number of particles with diameter d_i.

Rheological measurement

The rheological measurement was carried out on a stress controlled rheometer (AR 2000ex, USA) using a 20-mm diameter parallel plate. The sample disk was first prepared with a thickness of 1.0 mm and a diameter of 20 mm through a compression molding way at 200°C for 5 min. During the rheological measurement process, the frequency sweep from 0.01 to 100 rad s^{-1} was performed at 170°C under dry nitrogen atmosphere. For all the measurements, the samples were tested within the linear viscoelastic strain range.

Wide angle X-ray diffraction

The crystalline structures of samples were investigated using a wide angle X-ray diffraction (WAXD□Panalytical X'pert PRO diffractometer with Ni-filtered Cu Kα radiation, the Netherlands). The continuous scanning angle range used in this study was from 5° to 35° at 40 kV and 40 mA. Samples were obtained directly from the core zone of the injection-molded bars.

Differential scanning calorimetry

Differential scanning calorimetry (DSC, Netzsch STA 449C Jupiter, Germany) was used to investigate the cold crystallization and melting behaviors of the samples obtained from the injection-molded bars. A sample of about 8 mg was heated directly from room temperature (23°C) to 200°C at a heating rate of 10°C min^{-1}.

The values of X_c (%) of PLLA was calculated according to following equation:

$$X_c(\%) = \frac{\Delta H_m}{\Delta H_m^0 \times \phi} \times 100\% \tag{2}$$

where ΔH_m is the DSC-measured value of fusion enthalpy obtained during the heating process, ΔH_m^0 is the fusion enthalpy of the complete crystalline PLLA, and ϕ is the weight fraction of PLLA in the sample. Here, the value of ΔH_m^0 of PLLA was selected as 93 J g^{-1}.[30]

Polarization optical microscope

Polarization optical microscope (POM, Leica DMIP) equipped with a hot stage (Linkam) was used to characterize the crystalline morphologies obtained from isothermal crystallization process and annealing process, respectively. For the isothermal crystallization process, a sample of about 5 mg was placed between two glass slides and was heated to melt completely, and then the sample was pressed to obtain a slice with a thickness of about 20 μm. After that, the sample was transferred to the hot stage with a predetermined temperature of 105°C. For the annealed sample, the slice was heated to 200°C and maintained at this temperature for 5 min to erase any thermal history, then the sample was cooled down to room temperature in air. After that, the sample was placed in a fan-assisted oven at temperature of 80°C for 1 h.

Mechanical properties

Tensile properties of unannealed and annealed injection-molded bars were measured using a universal testing machine (AGS-J, SHIMADZU, China) at the tensile speed of 50 mm min^{-1} (23°C). Notched Izod impact strength was measured using an impact tester (XC-22Z, China) according to ISO180-2000. All the mechanical measurements were carried out at room temperature (23 ± 1°C). The average value reported was derived from at least five specimens.

RESULTS AND DISCUSSION

Phase morphologies

Figure 1 shows the phase morphologies of PLLA/EVA blends. As is well known to all, the phase morphologies of blends are mainly dependent on the composition, the processing condition, viscosity ratio, and interfacial interaction. Especially, the good

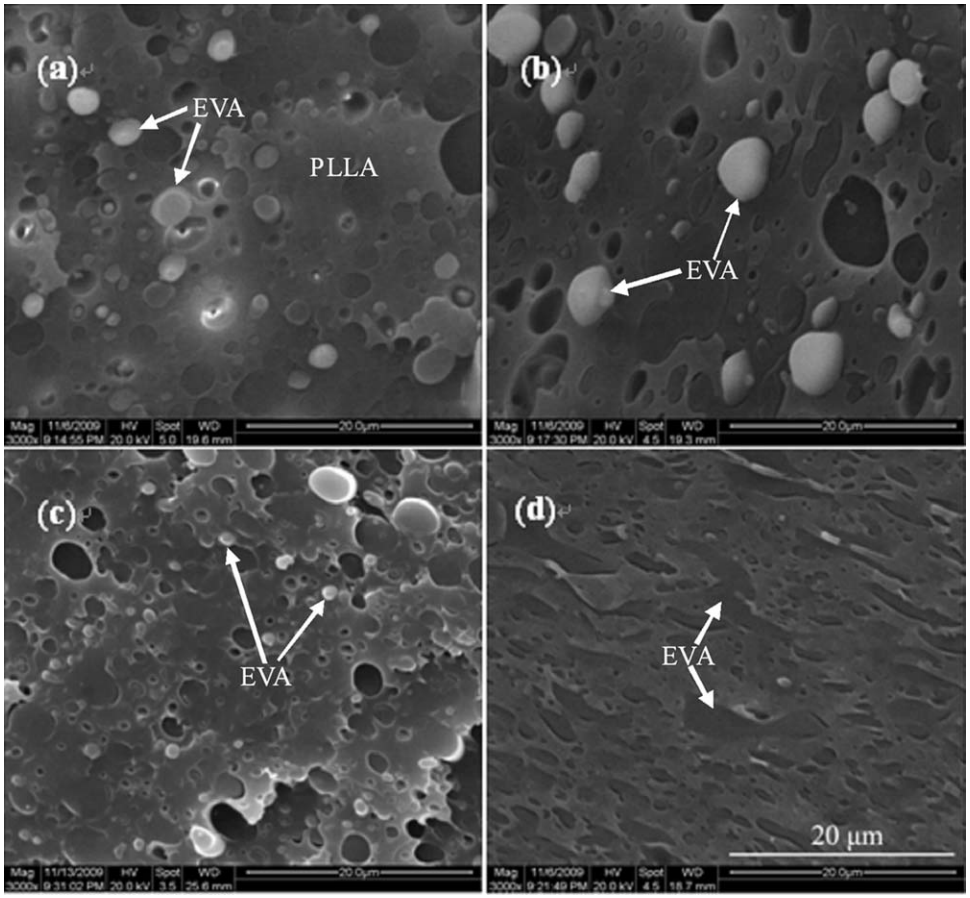

Figure 1 SEM images show the morphologies of PLLA/EVA (70/30) blend at different VA contents. The VA content is (a) 7.5 wt %, (b) 18 wt %, (c) 28 wt %, and (d) 40 wt %.

compatibility between the matrix and the dispersed phase is favorable to the homogeneous distribution of dispersed phase with smaller diameters. In this work, all the blends maintain the same composition, namely, PLLA/EVA = 70/30, and the processing condition is completely same. However, the blends of PLLA/7.5EVA, PLLA/18EVA, and PLLA/28EVA exhibit the typical sea-island morphology features: EVA is the dispersed phase and PLLA is the matrix (shown by arrows in the SEM images). For PLLA/40EVA, it exhibits an approximate co-continuous morphology feature. Furthermore, even for the sea-island morphologies, EVA exhibits the different particle diameters with the variation of VA content. The average particle diameters of EVA in PLLA/7.5EVA, PLLA/18EVA, and PLLA/28EVA are 2.95, 4.79, and 2.04 μm, respectively. 18EVA exhibits the biggest average diameter and 28EVA exhibits the smallest one. In other words, the SEM morphologies suggest that PLLA/28EVA shows better compatibility when compared with PLLA/7.5EVA and PLLA/18EVA. To visualize the interaction between PLLA and EVA, FTIR was applied, and the results are shown in Figure 2. From Figure 2, one can see that, with the presence of EVA, the absorption peak of γCH_3 + νCC (913 cm^{-1}) of PLLA disappears and the shape of absorption peaks of $\nu C = O$ (1751 cm^{-1}), $\delta sCH3$ (1373 cm^{-1}), and $\nu_{as}COC$ (1180 cm^{-1}) changes,[31] indicating the interaction between PLLA and EVA.

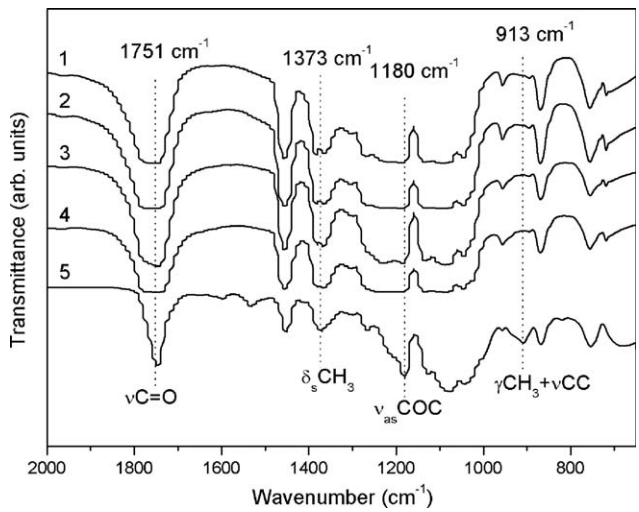

Figure 2 FTIR spectra of pure PLLA and PLLA/EVA (70/30) blend at different VA contents. The VA content is (1) 7.5 wt %, (2) 18 wt %, (3) 28 wt % and (4) 40 wt %, and (5) pure PLLA.

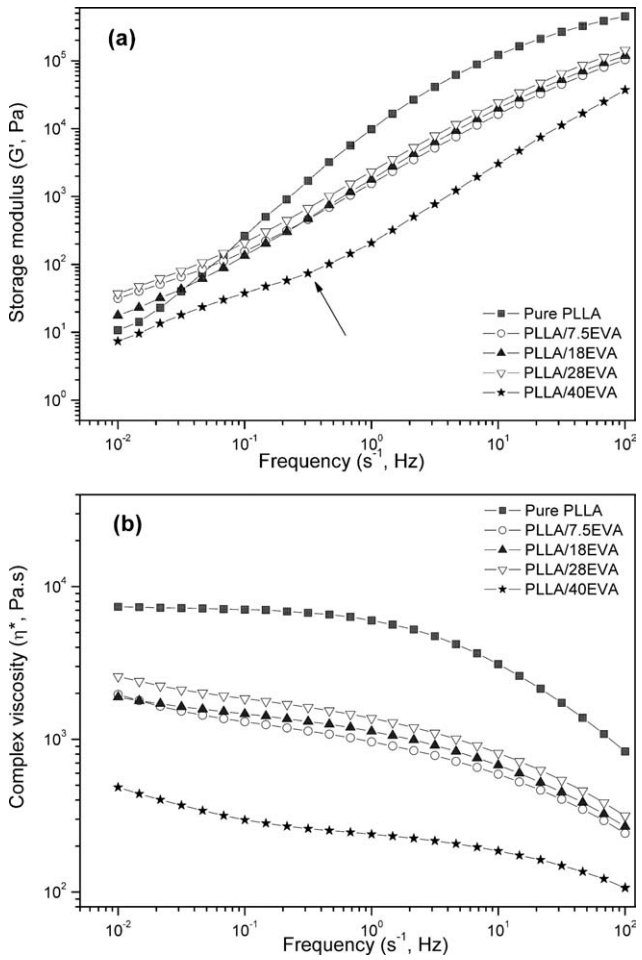

Figure 3 Rheological properties of PLLA/EVA melts at different VA contents. (a) Storage modulus (G') and (b) complex viscosity (η^*).

However, Figure 2 does not show the degree of the interaction of PLLA/EVA blends with the variation of VA content.

Rheological properties

Investigating on the rheological properties is favorable to the understanding of the processing of polymer blends. On the other hand, rheological properties also represent the interaction between phases and the morphologies of the blends.[32] From Figure 3 one can see that, the storage modulus (G') decreases with the increasing of VA content. As is well known, the crystallization behavior of EVA deteriorates, and the T_m, which is mainly relating to the lamellae thickness, decreases gradually with the increasing of VA content.[33] As shown in Table I, the T_m of pure EVA gradually decreases from 97°C of 7.5EVA to 58.8°C of 40 EVA. Thus, the dilution effect of EVA on PLLA becomes more apparent at higher VA content [seen in Fig. 3(b)], especially when the blend exhibits approximate co-continuous morphology feature. Furthermore, one can observe a shoulder on the storage modulus curve of the PLLA/40EVA blend (as shown by solid arrow). The similar phenomenon has been reported elsewhere for PLLA/ poly(ε-caprolactone) (PCL) blend, and the reason is attributed to the shape relaxation of the discrete PLLA phase induced by the addition of PCL.[34–36] Addition of PCL induces the presence of interface with long relaxation during oscillatory shear flow, which leads to an additional transition shoulder on the modulus curves. Obviously, the presence of the shoulder on the modulus curves observed in this work can be attributed to the addition of EVA with 40 wt % VA, which endows the blends, the approximate co-continuous morphology. From Figure 3(b), one can also see that pure PLLA exhibits the Newtonian plateau at relatively lower shear frequency. However, with the presence of EVA, the blends exhibits the viscosity curves with gradually developed slopes, namely, the typical feature of shear thinning behaviors, and no plateau regions can be observed over the studied frequency range. Especially, the decreased complex viscosity of PLLA/EVA means at least that, with the presence of EVA with lower viscosity, the processability of PLLA is improved apparently.

Figure 4 shows the results of storage modulus and complex viscosity versus VA content together with the same results calculated using mixing rule at angular frequency of 0.1 s^{-1}. It can be seen that, PLLA/28EVA blend exhibits maximum storage modulus and complex viscosity. The similar phenomena were reported by Razavi Aghjeh in investigating the effect of composition on rheological properties of PE/EVA blends,[37] and they claimed that the positive deviation of storage modulus and viscosity was induced by the strong interfacial interaction between PE and EVA. With the further variation of the composition from PE-rich to EVA-rich blends, the interfacial interaction weakens and negative deviation of storage modulus and viscosity was reported. According to the SEM results in Figure 1, in which PLLA/28EVA exhibits homogeneous and smallest dispersed particles, it can be suggested that the better compatibility between PLLA and 28EVA, possibly induced by the relatively stronger interfacial interaction, is the main reason for the homogeneous distribution of 28EVA in PLLA. For PLLA/40EVA, the compatibility should be better due to more polar groups presented in the EVA phase. However, the storage modulus and complex viscosity are smaller than those of PLLA/28EVA. This can be ascribed to the formation of the co-continuous morphology in PLLA/40EVA and the lower properties of the 40EVA simultaneously.

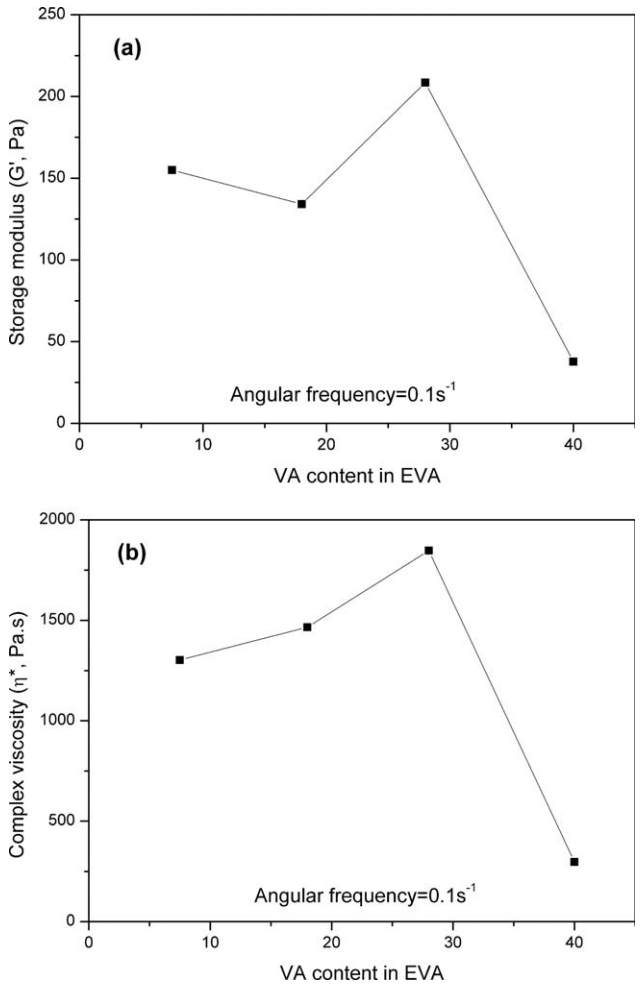

Figure 4 Variation of rheological properties of PLLA/EVA melts versus VA content. (a) Storage modulus (G') and (b) complex viscosity (η^*).

Crystallization behavior

Nonisothermal crystallization

The crystalline structures of injection-molded bars were investigated directly using WAXD and DSC, and the results are shown in Figures 5 and 6. In these measurements, the samples were cut from the core zones of the injection-molded bars. For pure PLLA, no visible diffraction peak attributed to crystalline structure is detected, indicating that the sample is completely amorphous or the amount of crystalline structure is very small to be traced by WAXD. For the blends, only two diffraction peaks at $2\theta = 21.3^\circ$ and 23.6°, corresponding to the diffractions of (110) and (200) planes of EVA phase, can be differentiated. Such diffractions weaken gradually with the increase of VA content, indicating that the crystallization of EVA becomes more difficult. Furthermore, PLLA is still in amorphous state. In other words, the presence of EVA does not influence the crystallization behavior of PLLA possibly due to the relatively fast cooling rate during the injection-molding processing.

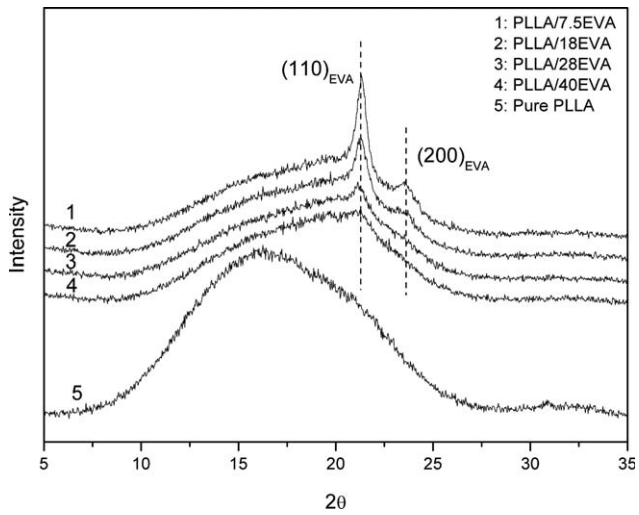

Figure 5 WAXD profiles of PLLA/EVA blends. Samples were obtained directly from the injection-molded bars.

Figure 6 shows the DSC heating curves of the samples cut from the injection-molded bars, and the corresponding parameters of PLLA are shown in Table II. It can be seen that the presence of EVA exhibits no apparent influence on the glass transition of PLLA ($T_{g\text{-PLLA}}$). The heating curve of pure PLLA is very smooth without any exothermic and/or endothermic peak possibly due to the relative high heating rate resulting in less time for the cold crystallization of pure PLLA.[28] For PLLA/EVA blends, the endothermic peaks ($T_{m\text{-EVA}}$) observed at relatively low temperatures (60–94°C) are attributed to the fusion of EVA lamellae. On the other hand, one can observe an exothermic peak ($T_{cc\text{-PLLA}}$) at about 125–128°C and an endothermic peak ($T_{m\text{-PLLA}}$) at

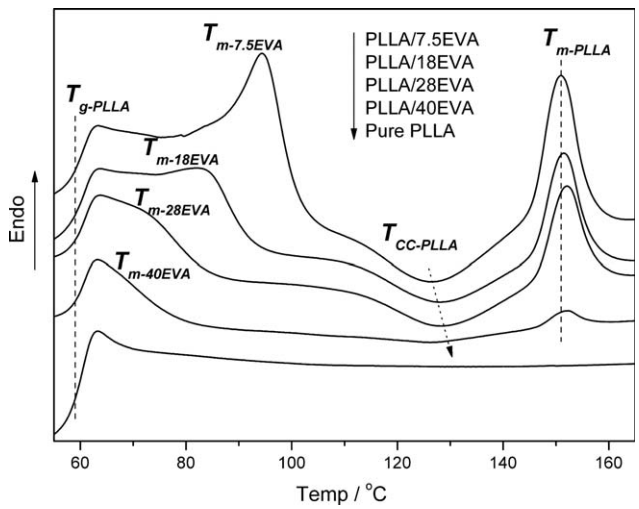

Figure 6 DSC heating curves of PLLA/EVA blends. Samples were obtained directly from the injection-molded bars.

TABLE II
Cold Crystallization and Subsequent Melting Parameters of PLLA Obtained from DSC Measurement

Samples	T_{cc} (°C)	ΔH_{cc} (J g^{-1})	T_m (°C)	ΔH_m (J g^{-1})	X_c (%)
Pure PLLA	–	–	–	–	–
PLLA/7.5EVA	125.9	−7.3	151.0	6.6	9.7
PLLA/18EVA	128.2	−5.0	151.4	4.8	7.4
PLLA/28EVA	128.2	−4.5	152.2	4.4	6.8
PLLA/40EVA	126.1	−1.0	151.9	0.6	0.9

Samples were obtained directly from injection-molded bars.

about 151–152°C, indicating the cold-crystallization and subsequent fusion of PLLA crystallites, respectively. With the increase of VA content, the exothermic peak weakens and shifts to higher temperatures slightly, which means that the cold crystallization of PLLA becomes more difficult, and less PLLA can transform into crystalline state. Consequently, the X_c (%) of PLLA decreases with the increase of VA content. The effects of VA content on cold-crystallization behavior of PLLA can be explained as follows. During the heating process, EVA melts first and possibly promotes the mobility of chain segments in the

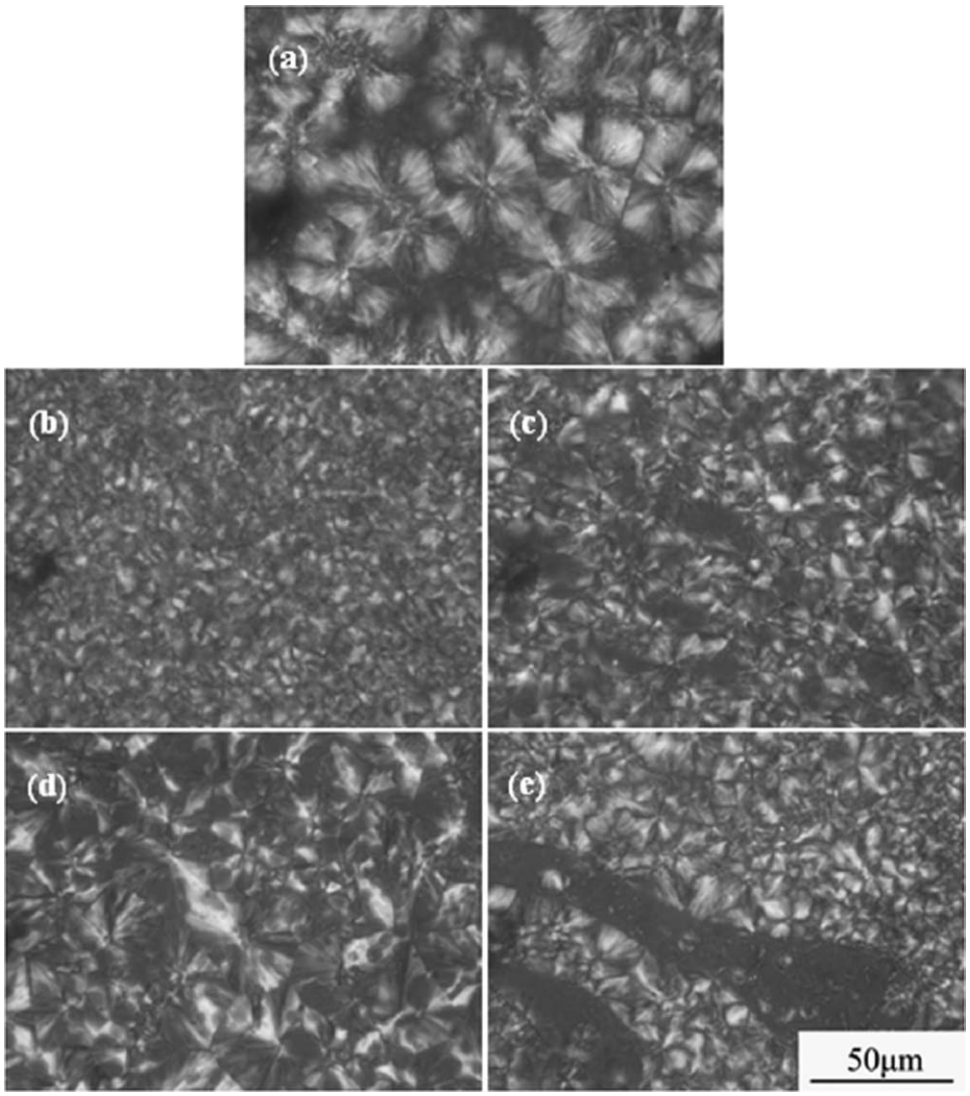

Figure 7 POM images show the isothermal crystallization morphologies of pure PLLA and PLLA/EVA blends obtained after isothermal crystallization at 105°C for 1 h. (a) Pure PLLA, (b) PLLA/7.5EVA, (c) PLLA/18EVA, (d) PLLA/28EVA, and (e) PLLA/40EVA.

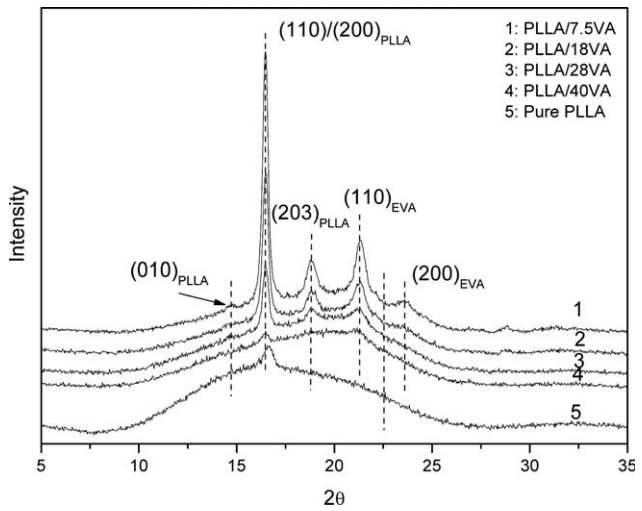

Figure 8 WAXD profiles of annealed PLLA/EVA blends. Samples were obtained from the injection-molded bars after being annealed at 80°C for 1 h.

interface between PLLA and EVA, showing the role of plasticizer in promoting the cold crystallization of PLLA.[29] However, the effect becomes inconspicuous with high content of VA monomer in EVA phase possibly due to the enhanced compatibility between PLLA and EVA, which prevents the migration of PLLA chain segments out from EVA phase, limits the crystallization of PLLA at this temperature and heating rate.

Isothermal crystallization morphologies

The isothermal crystallization behavior of the blends was visualized using POM, and the results are shown in Figure 7. Pure PLLA exhibits improved spherulites with an average diameter of approximately 40–50 μm. The addition of EVA promotes the increase of nucleation density and consequently, less improved spherulites with much smaller diameters are observed. Because the crystallization occurs at the temperature of 105°C, which is higher than the T_m of any EVA, it can be deduced that the role of EVA is mainly to promote the mobility of chain segments of PLLA, which is favorable to the nucleation and growth of PLLA spherulites.

Effect of annealing on crystalline structure

Figure 5 proves that PLLA is completely amorphous whether in pure PLLA or in the blends during the injection-molding processing, which is unfavorable to the improvement of the thermal properties of the particles. Thus, post-thermal treatment, that is annealing, was adopted in this work. The crystalline structures of annealed injection-molded bars were investigated using WAXD, and the results are shown in Figure 8. As shown in Figure 8, after being annealed at 80°C for only 1 h, pure PLLA exhibits a very weak diffraction peak at $2\theta = 16.6°$, attributing to the diffraction of (110)/(200) crystal planes of PLLA, indicating that there is a few amounts of PLLA crystallites forming during the annealing process. Interestingly, the blends exhibit different variation trends of the WAXD profiles. PLLA/7.5EVA exhibits very strong diffraction peak of (110)/(200) planes and new diffraction peaks of (010) and (203) planes, at $2\theta = 14.7°$ and 18.8°, respectively, also can be observed. Especially, the diffraction peaks of (110)/(200) planes of the blends shift to lower 2θ value, indicating the increase of d-spacing of PLLA lamellae with the presence of EVA. With the increase of VA content, the intensity of the diffraction peaks reduces dramatically, suggesting less PLLA crystallites forming during the annealing process. Especially, PLLA/40EVA exhibits weaker diffraction peak of (110)/(200) planes compared with

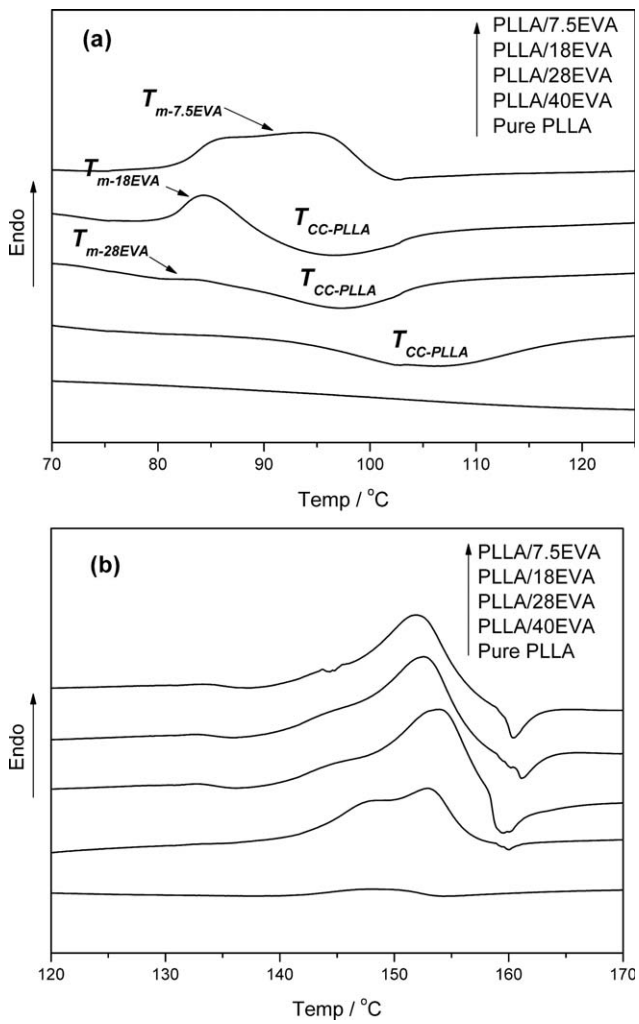

Figure 9 DSC heating curves of PLLA/EVA blends. Samples were obtained from the injection-molded bars after being annealed at 80°C for 1 h. (a) Cold crystallization and (b) melting behavior.

TABLE III
Cold Crystallization and Subsequent Melting Parameters Obtained from DSC Measurement

Samples	T_{cc} (°C)	ΔH_{cc} (J g^{-1})	T_m (°C)	ΔH_m (J g^{-1})	X_c (%)
Pure PLLA	–	–	148.2	1.2	1.3
PLLA/7.5EVA	–	–	152.0	23.0	35.4
PLLA/18EVA	95.7	−15.0	152.6	23.1	35.5
PLLA/28EVA	99.8	−11.1	154.1	24.7	37.9
PLLA/40EVA	107.0	−12.4	153.2	12.8	19.7

Samples were obtained after being annealed at 80°C for 1 h.

pure PLLA, which means that the second crystallization process of PLLA is prevented by 40EVA in this condition. To prove this, the annealed samples were further detected using DSC, and the results are shown in Figure 9 and Table III.

From Figure 9, one can see that, after being annealed, nearly no cold-crystallization behavior can be traced by DSC for pure PLLA. However, one can observe a very small endothermic peak at T_m of 148.2°C, relating to the X_c (%) of 1.3%. This agrees well with the results observed from WAXD measurement, which means that the second crystallization of pure PLLA is relatively difficult and only a few amounts of crystallites can be obtained. For PLLA/7.5EVA blend, the cold crystallization also disappears, and only a broad endothermic peak of 7.5EVA originated from the fusion of EVA phase at relatively lower temperature can be observed. However, an intense endothermic peak is observed at 152°C, and the X_c (%) is increased up to 35.4%, much higher than that of pure PLLA obtained in the same condition. This means that the fusion of PLLA is mainly originated from the crystallites formed during the annealing process. The disappearance of the cold crystallization of PLLA/7.5EVA during the DSC heating process is most likely due to that the crystallization of such sample is completely finished during the annealing process, and no PLLA further crystallizes during the DSC heating process. With the increase of VA content, the endothermic peak of EVA lamellae weakens and shifts to lower temperatures, because the crystallization of EVA chain segments becomes more difficult. Furthermore, one can observe apparent cold-crystallization phenomena occurring at T_{cc} of approximately 95–107°C, indicating the further crystallization of PLLA. Compared with the cold crystallization of the amorphous blends, which exhibit T_{cc} of approximately 125–128°C (Fig. 6), it can be deduced that the cold crystallization of annealed blends is easier than that of amorphous blends during the DSC heating process. This can be attributed to the promotion effect of PLLA crystallites formed during the annealing on the cold crystallization of amorphous PLLA during DSC heating process. Furthermore, a shoulder on the left side of the main endothermic peak can be differentiated for the annealed blends and higher T_m is achieved. It is believed that the shoulder is originated from the fusion of crystallites formed during the cold crystallization in DSC measurement, and the higher T_m from the fusion of crystallites with larger lamellae thickness formed during the annealing process. For PLLA/40EVA, the T_{cc} is much higher than that of PLLA/18EVA and PLLA/28EVA, indicating that the cold crystallization in this blend becomes more difficult. Furthermore, it shows much lower X_c (%). According to the WAXD measurement, it is easily believed that the endothermic peak of PLLA/40EVA is mainly related to the fusion of crystallites formed during the DSC heating process rather than during the annealing process.

The crystalline morphologies obtained during the annealing process were further detected using POM, and the representative results are shown in Figure 10. For pure PLLA, the crystallites are very few, which agrees well with the above results obtained by WAXD and DSC. For PLLA/7.5EVA blend, one can observe large amounts of fragments of crystallites. No improved spherulites can be differentiated, because the crystallization occurs in the condensed state rather than in the melt. The latter condition usually endows the chain segments enough time to enter into the lamellae with improved supermolecular structure, that is, spherulites.

The different effects of EVA with different VA contents on the crystallization of PLLA during the annealing process can be explained as follows. At lower VA content, PLLA and EVA are immiscible. However, the presence of VA chain segments exhibits interaction with PLLA to a certain extent, which locally activate the chain mobility of PLLA and promote the heterogeneous at the interface of 7.5EVA domains, resulting in large amounts of PLLA crystallites formation during the annealing process. With the increase of VA content, the interaction between PLLA and EVA is enhanced greatly, and it is believed that the blend is locally miscible, especially for PLLA/40EVA blend. Consequently, the presence of a large number of VA chain segments prevents the microphase separation of PLLA from EVA

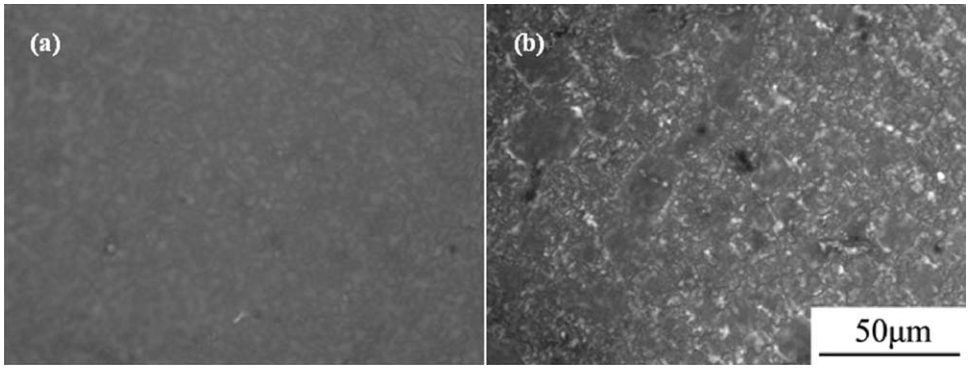

Figure 10 POM images show the typical crystalline morphologies of pure PLLA (a) and PLLA/7.5EVA (b) obtained after being annealed at 80°C for 1 h.

domains, preventing the nucleation and growth of PLLA crystallites. In other words, the limited miscibility between PLLA and EVA is favorable to the crystallization of PLLA. Similar work has been reported by Yazawa et al.,[11] and they observed that addition of 1 wt % PCL strongly promotes the nucleation of PLLA even if the aging temperature is lower than the glass transition temperature (T_g) of PLLA due to the locally improved miscibility at the interface of PCL domains.

Mechanical properties

The tensile strength and notched Izod impact strength of the injection-molded bars before and after being annealed were measured, and the results are shown in Table IV. As expected, the presence of EVA induces the decline of the tensile strength and tensile modulus. The tensile properties are greatly dependent on the VA content. PLLA/28EVA exhibits maximum tensile strength and ductility compared with other three blends possibly due to the relative stronger interaction between PLLA and 28EVA as suggested by rheological properties on the one hand. On the other hand, PLLA/28EVA exhibits homogeneous distribution of EVA particles with much smaller diameters when compared with PLLA/7.5EVA and PLLA/18EVA blends, which is possibly the other reason for the improved tensile strength and ductility. For PLLA/40EVA, the sample exhibits the co-continuous morphology feature, and, consequently, the continuous 40EVA ligaments exhibit great role in determining the tensile strength. The impact strength increases linearly with the increase of VA content, suggesting the gradually improved toughening effect of EVA. Factually, EVA exhibits more characteristics of elastomer with more VA content: For 7.5EVA, it has large amounts of crystalline structure and acts as the role of semicrystalline plastic; for 40EVA; the crystallization of EVA chain segments becomes more difficult, and it exhibits the role of elastomer, which exhibits apparent toughening effect for PLLA. On the other hand, for the blends with typical sea-island morphologies, PLLA/28EVA exhibits much smaller particle diameter compared with PLLA/7.5EVA and PLLA/18EVA. It is well known to all, for the elastomer-toughened polymers, the smaller the particle diameter is, the better the toughening effect is.[17] For PLLA/40EVA, the blend exhibits the approximate co-continuous morphology, which is believed to be the other reason for the increased impact strength.[38] By the way, the mechanical properties of PLLA/18EVA are sometimes between PLLA/7.5EVA and PLLA/28EVA, but sometimes they are not. This is possibly attributes to the different roles of phase morphologies and the interfacial interaction in determining the different mechanical behaviors. After being annealed, the tensile strength and modulus are enhanced greatly, whereas the elongation at

TABLE IV
Mechanical Properties of PLLA and PLLA/EVA Blends Before and After Being Annealed at 80°C for 1 h

	Elastic modulus (MPa)		Tensile strength (MPa)		Elongation at break (%)		Impact strength (kJ m^{-2})	
Samples	Unannealed	Annealed	Unannealed	Annealed	Unannealed	Annealed	Unannealed	Annealed
Pure PLLA	1780 ± 112	2355 ± 51	66.0 ± 0.5	81.5 ± 6.3	5.7 ± 0.2	4.2 ± 0.1	2.7 ± 0.6	3.5 ± 0.6
PLLA/7.5VA	1342 ± 41	1842 ± 15	37.1 ± 0.4	45.1 ± 1.0	6.4 ± 0.1	4.3 ± 0.3	5.5 ± 0.5	5.7 ± 0.3
PLLA/18VA	1341 ± 35	1594 ± 24	33.3 ± 1.2	41.0 ± 0.8	10.8 ± 1.0	8.3 ± 0.6	6.2 ± 0.2	4.5 ± 0.2
PLLA/28VA	1330 ± 32	1827 ± 23	39.3 ± 0.6	47.3 ± 0.5	18.3 ± 2.1	12.3 ± 0.5	8.3 ± 0.6	6.9 ± 0.4
PLLA/40VA	1133 ± 27	1558 ± 32	27.7 ± 1.4	38.9 ± 1.1	12.0 ± 1.3	9.7 ± 0.2	11.8 ± 1.0	8.9 ± 0.3

break and impact strength are reduced slightly. For example, annealed PLLA/28EVA sample exhibits higher modulus and fracture toughness compared with the untreated pure PLLA, suggesting the improvement of stiffness and toughness simultaneously. In other words, through adjusting the composition and the application of post-thermal treatment, PLLA blends with comprehensive mechanical properties are achieved.

CONCLUSIONS

In summary, PLLA/EVA blends with different VA contents in EVA phase have been prepared. SEM images show that at lower VA content (7.5, 18, and 28 wt %), the blends exhibit the typical sea-island morphology features, whereas PLLA/40EVA exhibits the approximate co-continuous morphology feature. The stronger interfacial interaction in PLLA/28EVA, which exhibits homogeneous and smaller dispersed particle size, is suggested by the rheological results. All the samples exhibit the amorphous state during the injection molding process. However, post-thermal treatment (annealing) is favorable to the nucleation and second-crystallization of PLLA. Especially, the content of VA influences greatly the second crystallization of PLLA during the annealing process. Limited miscibility is proved to be favorable to the nucleation and crystalline improvement of PLLA. With the addition of EVA, the ductility and fracture toughness are enhanced. The decreased tensile modulus and strength can be enhanced by annealing.

Dr Wei Yang (Sichuan University) is appreciated greatly for the measurement of rheological properties.

References

1. Tsuji, H.; Ikada, Y. Polymer 1995, 36, 2709.
2. Pluta, M. Polymer 2004, 45, 8239.
3. Kulinski, Z.; Piorkowska, E. Polymer 2005, 46, 10290.
4. Martin, O.; Averous, L. Polymer 2001, 42, 6209.
5. Yu, L.; Liu, H.; Dean, K.; Chen, L. J Polym Sci Part B: Polym Phys 2008, 46, 2630.
6. Xiao, X.; Lu, W.; Yeh, J. T. J Appl Polym Sci 2009, 113, 112.
7. Lemmouchi, Y.; Murariu, M.; Santos, A. M. D.; Amass, A. J.; Schacht, E.; Dubois, P. Eur Polym J 2009, 45, 2839.
8. Anderson, N. S.; Schreck, K. M.; Hillmyer, M. A. Polym Rev 2008, 48, 85.
9. Zhang, L. L.; Goh, S. H.; Lee, S. F. Polymer 1998, 39, 4841.
10. Li, S. H.; Woo, E. M. Polym Int 2008, 57, 1242.
11. Sakai, F.; Nishikawa, K.; Inoue, Y.; Yazawa, K. Macromolecules 2009, 42, 8335.
12. Leung, B. O.; Hitchcock, A. P.; Brach, J. L.; Scholl, A.; Doran, A. Macromolecules 2009, 42, 1679.
13. Wu, D. F.; Zhang, Y. S.; Zhang, M.; Zhou, W. D. Eur Polym J 2008, 44, 2171.
14. Zhang, Y. S.; Wu, D. F.; Zhang, M.; Zhou, W. D.; Xu, C. C. Polym Eng Sci 2009, 49, 2293.
15. Ko, S. W.; Hong, M. K.; Park, B. J.; Gupta, R. K.; Choi, H. J.; Bhattacharya, S. N. Polym Bull 2009, 63, 125.
16. Gu, S. Y.; Zhang, K.; Ren, J.; Zhan, H. Carbohydr Polym 2008, 74, 79.
17. Ishida, S.; Nagasaki, R.; Chino, K.; Dong, T.; Inoue, Y. J Appl Polym Sci 2009, 113, 558.
18. Li, Y. J.; Shimizu, H. Eur Polym J 2009, 45, 738.
19. Tsuji, H.; Ikada, Y. Polymer 1995, 36, 2709.
20. Anderson, K. S.; Lim, S. H.; Hillmyer, M. A. J Appl Polym Sci 2003, 89, 3757.
21. Anderson, K. S.; Hillmyer, M. A. Polymer 2004, 45, 8809.
22. Gajria, A. M.; Davé, V.; Gross, R. A.; McCarthy, S. P. Polymer 1996, 37, 437.
23. Yoon, J. S.; Oh, S. H.; Kim, M. N.; Chin, I. J.; Kim, Y. H. Polymer 1999, 40, 2303.
24. Pan, P.; Zhu, B.; Inoue, Y. Macromolecules 2007, 40, 9664.
25. Yu, L.; Liu, H. S.; Xie, F. W.; Chen, L.; Li, X. X. Polym Eng Sci 2008, 48, 634.
26. Pan, P.; Zhu, B.; Kai, W.; Dong, T.; Inoue, Y. Macromolecules 2008, 41, 4296.
27. Na, B.; Tian, N.; Lv, R.; Zou, S.; Xu, W.; Fu, Q. Macromolecules 2010, 43, 1156.
28. Li, Y. L.; Wang, Y.; Liu, L.; Han, L.; Xiang, F. M.; Zhou, Z. W. J Polym Sci Part B: Polym Phys 2009, 47, 326.
29. Li, Y. L.; Wu, H. Y.; Wang, Y.; Liu, L.; Han, L.; Wu, J.; Xiang, F. M. J Polym Sci Part B: Polym Phys 2010, 48, 520.
30. Schmidt-Rohr, K.; Hu, W.; Zumbulyadis, N. Science 1998, 280, 714.
31. Kister, G.; Cassanas, G.; Vert, M. Polymer 1998, 39, 267.
32. Ajji, A.; Utracki, L. A. Polym Eng Sci 1996, 36, 1574.
33. Peeterbroeck, S.; Breugelmans, L.; Alexandre, M.; BNagy, J.; Viville, P.; Lazzaroni, R.; Dubois, P. Compos Sci Technol 2007, 67, 1659.
34. Wu, D. F.; Zhang, Y.; Zhang, M.; Yu, W. Biomacromolecules 2009, 10, 417.
35. Lee, H. M.; Park, O. O. J Rheol 1994, 38, 1405.
36. Yu, W.; Bousmina, M.; Grmela, M.; Zhou, C. X. J Rheol 2002, 46, 1401.
37. Faker, M.; Razavi Aghjeh, M. K.; Ghaffari, M.; Seyyedi, S. A. Eur Polym J 2008, 44, 1834.
38. Cho, K.; Seog, J.; Ahn, T. O. Polymer 1996, 37, 1541.